Journal of Medicinal Chemistry

Article

pubs.acs.org/jmc

# Structure–Activity Relationships, Ligand Efficiency, and Lipophilic Efficiency Profiles of Benzophenone-Type Inhibitors of the Multidrug Transporter P-Glycoprotein

Ishrat Jabeen,[†] Karin Pleban,[†] Uwe Rinner,[‡] Peter Chiba,[§] and Gerhard F. Ecker*[,†]

[†]University of Vienna, Department of Medicinal Chemistry, Althanstrasse 14, 1090, Vienna, Austria

[‡]University of Vienna, Department of Organic Chemistry, Währingerstrasse 38, 1090, Vienna, Austria

[§]Medical University of Vienna, Institute of Medical Chemistry, Währingerstrasse 10, 1090, Vienna, Austria

Supporting Information

**ABSTRACT:** The drug efflux pump P-glycoprotein (P-gp) has been shown to promote multidrug resistance (MDR) in tumors as well as to influence ADME properties of drug candidates. Here we synthesized and tested a series of benzophenone derivatives structurally analogous to propafenone-type inhibitors of P-gp. Some of the compounds showed ligand efficiency and lipophilic efficiency (LipE) values in the range of compounds which entered clinical trials as MDR modulators. Interestingly, although lipophilicity plays a dominant role for P-gp inhibitors, all compounds investigated showed LipE values below the threshold for promising drug candidates. Docking studies of selected analogues into a homology model of P-glycoprotein suggest that benzophenones show an interaction pattern similar to that previously identified for propafenone-type inhibitors.

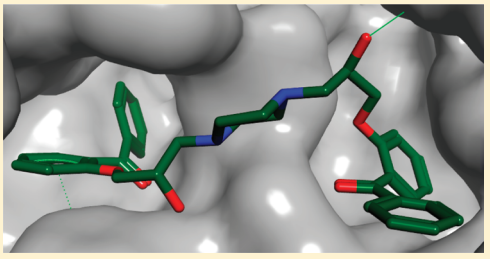

## INTRODUCTION

Membrane transporters are increasingly recognized for playing a key role in safety profiles of drug candidates, predominantly by their involvement in drug–drug interactions.[1,2] One of the most intensively studied families in this context is the ATP-binding cassette (ABC) transporter superfamily.[3−5] Several members of these ATP-driven transporters are expressed at tissue barriers and thus influence uptake and elimination of drugs and drug candidates.[6] Originally they have been linked to development of multidrug resistance (MDR) in tumor therapy, as they transport a wide variety of natural product toxins such as anthracyclines, vincristine, and taxanes out of tumor cells.[7,8] Thus, P-glycoprotein (P-gp/ABCB1), discovered in 1976 and considered the paradigm ABC transporter,[9,10] shows a remarkably broad substrate pattern, transporting numerous structurally and functionally diverse compounds across cell membranes.[3] P-gp is expressed at the blood–brain barrier (BBB), the blood–cerebrospinal fluid (B-CSF) barrier, and the intestinal barrier, thus modulating the absorption and excretion of xenobiotics across these barriers.[6] P-gp and its ligands (substrates and inhibitors) are therefore extensively studied both with respect to reversing multidrug resistance in tumors and for modifying ADME-Tox properties of drug candidates,[11] such as central nervous system (CNS) active agents.[12,13] Within the past two decades, numerous modulators of P-gp mediated drug efflux have been identified[14,15] and several entered clinical studies up to phase III. However, up to now no compound achieved approval, which is mainly due to severe side effects and lack of efficacy. This further emphasizes the physiological role of efflux transporters in general and P-gp in particular[16] and stresses the need for a more detailed knowledge on the structure and function of these proteins and the molecular basis of their interaction with small molecules.[17] The latter has been approached by numerous SAR and QSAR studies, which revealed that high lipophilicity seems to be a general prerequisite for high P-gp inhibitory potency, valid across different chemical scaffolds. This is also in line with recent structure-based studies, which indicate an entry pathway via the membrane bilayer.[18,19]

In recent years the concepts of "*Binding energy of the ligand per atom*" or ligand efficiency (LE)[20−22] and lipophilic efficiency (LipE),[23,24] which combines both "*potency and lipophilicity*," have been shown to be useful tools in the lead optimization process.[25,26] In the light of our extensive SAR and QSAR studies on propafenone analogues[27,28] (Figure 1) and related compounds, we also utilized benzophenone-based probes, which contain a photoactive arylcarbonyl group as part of the pharmacophore. This led to the identification of key amino acid residues interacting with these ligands.[29,30] Within this study, we extended the set of benzophenones in order to identify compounds with higher potency, utilizing also the concepts of LE and LipE. In addition, docking studies of selected compounds into a homology model of P-gp were performed to shed light on the potential binding mode of these compounds and to compare it with the binding hypothesis derived for analogous propafenones.[17]

**Received:** December 19, 2011
**Published:** March 27, 2012

  

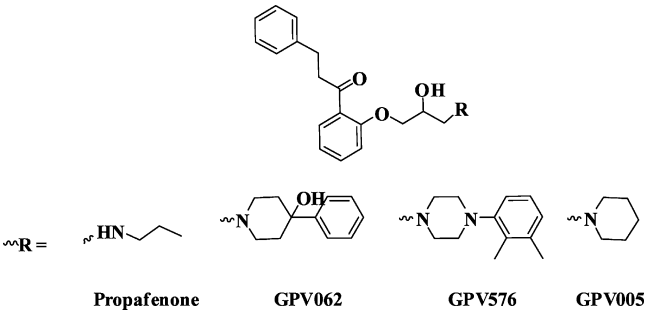


**Figure 1.** Selected propafenone analogues used in this study.

## RESULTS AND DISCUSSION

**Chemistry.** Synthesis of benzophenone analogues **6**–**24** was carried out in analogy to the synthesis of propafenone derivatives.[27] Briefly, the respective *ortho*-, *meta*-, or *para*-hydroxy benzophenone (**1a**–**c**) was alkylated with epichlorohydrine yielding *ortho*-, *meta*-, and *para*-oxiranes **2a**–**c**. Subsequent nucleophilic oxirane ring-opening with primary or secondary amines (R1) gave target compounds **6**–**19**. Excessive amount of oxirane **2a** upon nucleophilic ring-opening with piperazine yielded the homodimer **23**, whereas equimolar amounts of both partners predominantly gave the piperazine analogue **5** (Scheme 1).

Further treatment of piperazine analogue **5** with phenylisocyanate and its thio-analogue as described by Pitha et al.[31] yielded **21** and **22**, respectively. *O*-Alkylation of 2-hydroxy-5-methyl acetophenone (**3**) with epichlorohydrine yielded **4**, which, upon subsequent nucleophilic ring-opening by piperazine **5** yielded the heterodimer **24** (Scheme 2).

**Biological Activity.** Biological activity of target compounds **6**–**24** was assessed using the daunorubicin efflux protocol as described previously.[32] Briefly, multidrug resistant CCRF-CEM vcr 1000 cells were preloaded with daunorubicin and efflux was monitored by time-dependent decrease in mean cellular fluorescence in the absence and presence of various concentrations of compounds. $IC_{50}$ values were calculated from concentration–response curves derived from first-order rate constant of transport (i.e.$V_{max}/K_m$) as a function of compound concentration.[32] Thus, the effect of different modulators on the transport rate is measured in a direct functional assay. Values are given in Table 1 and are the mean of at least three independently performed experiments. Generally, interexperimental variation was below 20%.

**Structure–Activity Relationships.** Table 1 shows the P-gp inhibitory potency of compounds **6**–**24**. The $IC_{50}$ values cover a broad range, spanning from 0.05 $\mu$M for the dimer **23** up to 13.37 $\mu$M for the morpholine analogue **15**. Besides the *ortho*-benzophenone dimer **23**, also the ortho analogues showing an arylpiperazine moiety (**6**, **9**) are highly active. Interestingly, the heterodimer **24** is one of the least active compounds in the data set, together with the morpholine derivatives **15** and **16**. With respect to substitution pattern at the central aromatic benzene moiety, the rank order for arylpiperazine substituted compounds generally is ortho > meta > para. An analogous trend has also been observed for propafenone analogues.[33] However, for compounds bearing piperidine or morpholine moieties, this trend is partly reversed. In the case of piperidine derivatives, the para-derivative is slightly more active than the meta analogue (1.20 vs 3.55 vs 2.18). Interestingly, also for the morpholine analogues, the para-derivative is by a factor of 2 more active than ortho-derivative ($P$ = 0.01). Thus, the influence of the substitution pattern at the central aromatic ring seems to be more pronounced if the vicinity of the nitrogen comprises large, lipophilic moieties. This is in line with our previous findings using hydrophobic moments as descriptors in QSAR studies.[34]

To assess the role of lipophilicity as a general predictor for high potency, we also calculated logP values using the software Bio-Loom version 1.5[35] and correlated them with $pIC_{50}$ values (Figure 2). Boi-Loom, which calculates logP values by a fragment-based approach, was validated against experimental logP values by Sakuratani et al.[36] The $r^2$ value of 0.56 indicates that also in the series of benzophenones biological activity increases with the lipophilicity of the compounds. This is in agreement with the notion that compounds most probably enter the binding cavity of P-gp directly from the membrane bilayer.[18] This is additionally supported by the recent X-ray structure of mouse P-gp, which shows a large inner cavity accessible from the membrane via putative entry ports composed of transmembrane helices 4/6 on one side and 10/12 on the other side.[19]

The 4-hydroxy-4-phenyl-piperidine analogue **19** is located above the clogP/$pIC_{50}$ correlation line ($pIC_{50}$, 5.76 calcd vs 6.51 obs), which further confirms our previous results on the

**Scheme 1**[a]

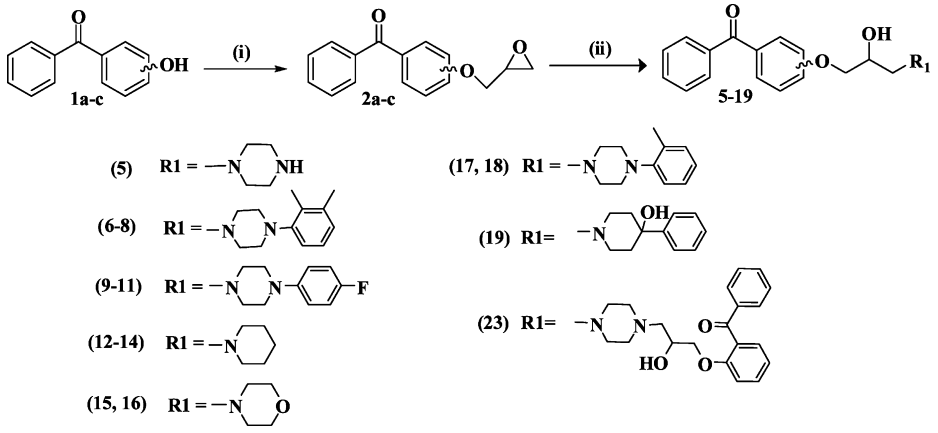


[a]Reagents and conditions: (i) NaOH, epicholorohydrine, reflux for 24 h; (ii) methanol, respective amine (R1), reflux for 24 h (**5**–**19**, **23**).


dx.doi.org/10.1021/jm201705f | J. Med. Chem. 2012, 55, 3261–3273

**Scheme 2**[a]

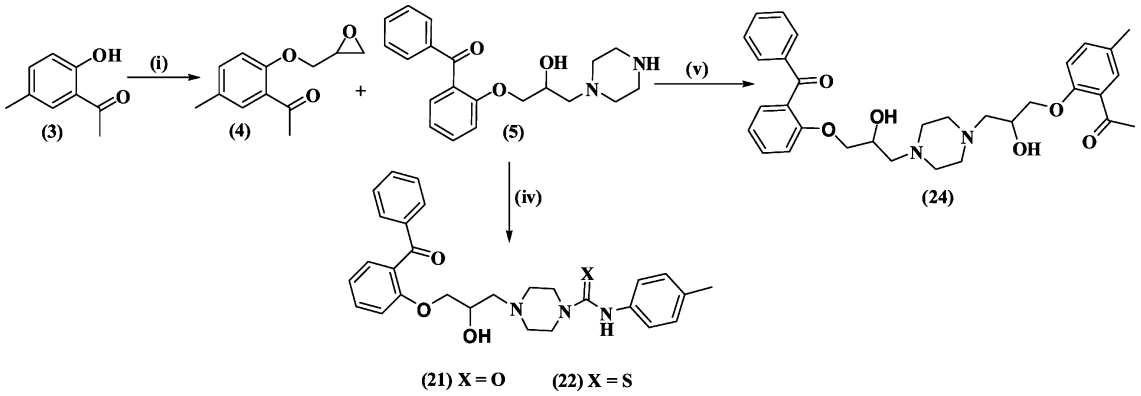


[a]Reagents and conditions: (i) NaOH, epicholorohydrine, reflux for 24 h; (iv) *p*-tolyl isocyanate, $CH_2Cl_2$, stirring 2 h (X = O), *p*-tolylisothiocyanate, $CH_2Cl_2$, stirring 2 h (X = S); (v) methanol, reflux 5 h.

**Table 1. Chemical Structure, Ligand Efficiency (LE), Lipophilic Efficiency (LipE), and Pharmacological Activity of Compounds 6−24**

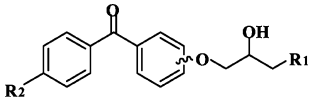

| Comp | Position[a] | $R_1$ | $R_2$ | $IC_{50}$ (μM)± SEM | LE | LE_Scale | clogP | LipE |
|---|---|---|---|---|---|---|---|---|
| **6** | Ortho |  | H | 0.08 ± 0.01 | 0.30 | 0.30 | 5.52 | 1.58 |
| **7** | Meta |  | H | 0.17 ± 0.18 | 0.29 | 0.30 | 5.52 | 1.24 |
| **8** | Para |  | H | 0.65 ± 0.08 | 0.26 | 0.30 | 5.52 | 0.66 |
| **9** | Ortho | 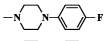 | H | 0.15 ± 0.03 | 0.30 | 0.30 | 4.96 | 1.86 |
| **10** | Meta | 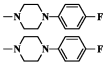 | H | 0.58 ± 0.02 | 0.28 | 0.30 | 4.96 | 1.27 |
| **11** | Para |  | H | 0.97 ± 0.02 | 0.27 | 0.30 | 4.96 | 1.04 |
| **12** | Ortho |  | H | 1.20 ± 0.36 | 0.33 | 0.36 | 3.88 | 2.04 |
| **13** | Meta |  | H | 3.55 ± 0.08 | 0.31 | 0.36 | 3.88 | 1.57 |
| **14** | Para |  | H | 2.18 ± 0.07 | 0.32 | 0.36 | 3.88 | 1.78 |
| **15** | Ortho |  | H | 13.37 ± 1.18 | 0.28 | 0.36 | 2.66 | 2.21 |
| **16** | Para |  | H | 5.32 ± 0.89 | 0.30 | 0.36 | 2.66 | 2.61 |
| **17** | Meta |  | H | 0.20 ± 0.01 | 0.30 | 0.30 | 5.07 | 1.62 |
| **18** | Para |  | H | 0.50 ± 0.08 | 0.28 | 0.30 | 5.07 | 1.23 |
| **19** | Ortho |  | H | 0.31 ± 0.00 | 0.29 | 0.30 | 3.65 | 2.86 |
| **20**[29] | Ortho |  | $CH_3$ | 1.21 ± 0.18 | 0.35 | 0.37 | 3.64 | 2.28 |
| **21** | Ortho | 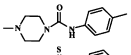 | H | 0.48 ± 0.01 | 0.26 | 0.28 | 4.28 | 2.04 |
| **22** | Ortho | 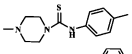 | H | 0.38 ± 0.01 | 0.26 | 0.28 | 5.07 | 1.34 |
| **23** | Ortho | 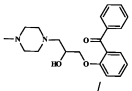 | H | 0.05 ± 0.00 | 0.23 | 0.23 | 4.27 | 3.01 |
| **24** | Ortho | 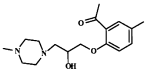 | H | 9.48 ± 0.18 | 0.18 | 0.25 | 3.17 | 1.85 |

[a]Position of the side chain at central aromatic ring.

importance of the 4-hydroxy-4-phenyl-piperidine moiety for high biological activity of propafenone derivatives.[37] These results were recently supported by extensive docking studies of propafenone analogues.[17] It is also interesting to note that the homodimer **23** is about one log unit more potent than predicted by the clogP/$pIC_{50}$ plot ($pIC_{50}$, 6.10 calcd vs 7.27 obs). A pairwise comparison of equilipophilic compounds **23** vs **21** (clogP, 4.27 vs 4.28; $IC_{50}$, 0.05 vs 0.48 μM) and **19** vs **20** (clogP, 3.65 vs 3.64; $IC_{50}$, 0.31 vs 1.21 μM) indicates that mutual activity differences might also be due to difference in molecular size. The dimer **23** (44 heavy atoms) is about 1 order of magnitude more active then **21** (35 heavy atoms). Similarly, **19** (32 heavy atoms) is about a factor of 4 more active than **20** (24 heavy atoms). This also points toward a commonly observed phenomenon in lead optimization programs, i.e., activity increases with the size of the molecules. Therefore, ligand efficiency (LE)[20−22] and lipophilic efficiency (LipE)[23,24] profiles of inhibitors/substrates of P-gp have been used to


dx.doi.org/10.1021/jm201705f | J. Med. Chem. 2012, 55, 3261−3273

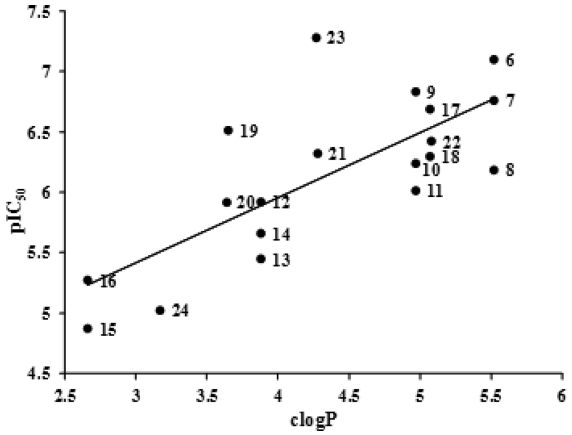


**Figure 2.** Correlation of P-gp inhibitory potency of compounds **6**–**24** (expressed as $pIC_{50}$ values) vs calculated logP values of the ligands.

identify the derivatives with the best activity/size (or logP) ratio, which should provide further insights for the design of new ligands.[25,26]

*Ligand Efficiency (LE).* LE, most commonly defined as the ratio of free energy of binding to the number of heavy atoms, is a simple metric for assessing whether a ligand derives its potency from optimal fit with the target protein or simply by virtue of making many contacts.[38] To get more information on the most promising P-gp inhibitors and to compare them to well established P-gp inhibitors/substrates, we calculated ligand efficiency values of benzophenones **6**–**24**, selected propafenone analogues (Figure 1), as well as P-gp inhibitors which entered clinical studies. Ligand efficiencies were calculated as described in the Materials and Methods section. For benzophenones, small ligands such as the *N*-propyl derivative **20** and the piperidine analogue **12** show higher efficiency values (0.35; 0.33) than the large dimers **23** and **24** (0.23; 0.18). For the whole data set, it can be observed that ligand efficiencies drop dramatically when the size of the ligands increases above 50 heavy atoms (Figure 3).

A similar trend has been observed in the literature, with LE showing generally a dependency on ligand size.[21] As LE in principle is supposed to normalize for the size of the ligand, various proposals have been made to solve this problem.[22,39] As the heavy atom count of the ligands in our data set varies from 24 to 86 (**20**; valspodar), LE values were subsequently scaled as

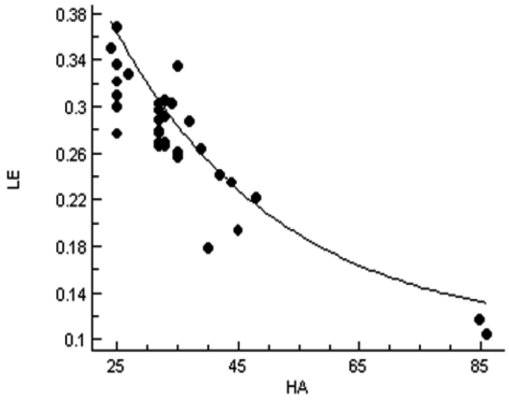


**Figure 3.** Plot of ligand efficiency vs heavy atom count for benzophenone analogues, compounds which entered clinical studies and selected propafenones.

described by Reynolds et al.[21,22] to retrieve a size-independent ligand efficiency value (LE_Scale). This was achieved by fitting the top ligand efficiency versus heavy atom count to a simple exponential function, as outlined by Reynolds et al.,[21] (eq 1; Figure 3). Subsequently, the ratio of ligand efficiency over normalized ligand efficiency scale gives a scoring function called "Fit Quality" (FQ) (eq 2). According to Reynolds et al., fit quality scores close to 1.0 or above indicate near optimal ligand binding, while low fit quality scores are indicative of suboptimal binding.

$$\text{LEScale} = 0.104 + 0.65e^{-0.037*HA} \quad (1)$$

$$\text{FQ} = \text{LE}/\text{LEScale} \quad (2)$$

Use of this criterion shows that most of the compounds under clinical investigation show FQ scores above 1, including zosuquidar, ONT093, elacridar, and tariquidar, along with benzophenones **6** and **23**, as well as propafenone and its analogues GPV062 and GPV576 (Figure 4; Table 2).

It is interesting to note that especially those compounds which were specifically designed as P-gp inhibitors (ONT093, zosuquidar, elacridar, tariquidar) show higher FQ values than those originating from drug repurposing attempts (verapamil, cyclosporine, and its analogue valspodar). With respect to propafenone analogues, GPV576 is the hitherto most active analogue we synthesized showing a highly lipophilic but quite compact substituent at the nitrogen atom (4-tolylpiperazine). Interestingly, the top ranked benzophenone analogue **6** also has a 4-tolylpiperazine moiety. This might point toward the tolylpiperazine substituent for being a privileged substructure for P-gp inhibitors. GPV062 bears a 4-hydroxy-4-phenylpiperidine moiety, which has been shown to influence biological activity independent of lipophilicity, resulting in an almost 10-fold increase of inhibitory potency when compared to compounds having other substituents at the nitrogen atom. This points toward a distinct additional interaction mediated by the 4-hydroxy group, most probably in the form of a hydrogen bond. Finally, propafenone itself shows a very good value, thus retrospectively demonstrating its validity as starting point for structural modifications. However, it should be noted that during its catalytic cycle the transporter undergoes a major conformational change and that it might well be that some inhibitors exert their effect by slow off kinetics rather than by strong binding to the apo state. In this case, LE values derived from $IC_{50}$ values for transport inhibition should be taken cautiously.

As already outlined, lipophilicity has been shown in numerous studies to be a general predictor for high P-gp inhibitory potency. This most probably is due to the proposed access path of the compounds, which seems to be directly from the membrane bilayer. On the other hand, high lipophilicity is very often associated with poor oral drug-like properties. This led to the assumption that clogP values between 2 and 3 are considered optimal in an oral drug program and prompted Leeson et al., to introduce the concept of lipophilic efficiency.[23]

*Liphophilic Efficiency (LipE).* LipE is a parameter that combines both potency and lipophilicity and is defined as a measure of how efficiently a ligand exploits its lipophilicity to bind to a given target. Briefly, in a lead optimization series, there is a greater likelihood of achieving good in vivo performance when potency can be increased without increasing logP or logD values. To explore this concept also for P-gp inhibitors, we calculated LipE values for the whole set of


dx.doi.org/10.1021/jm201705f | J. Med. Chem. 2012, 55, 3261–3273

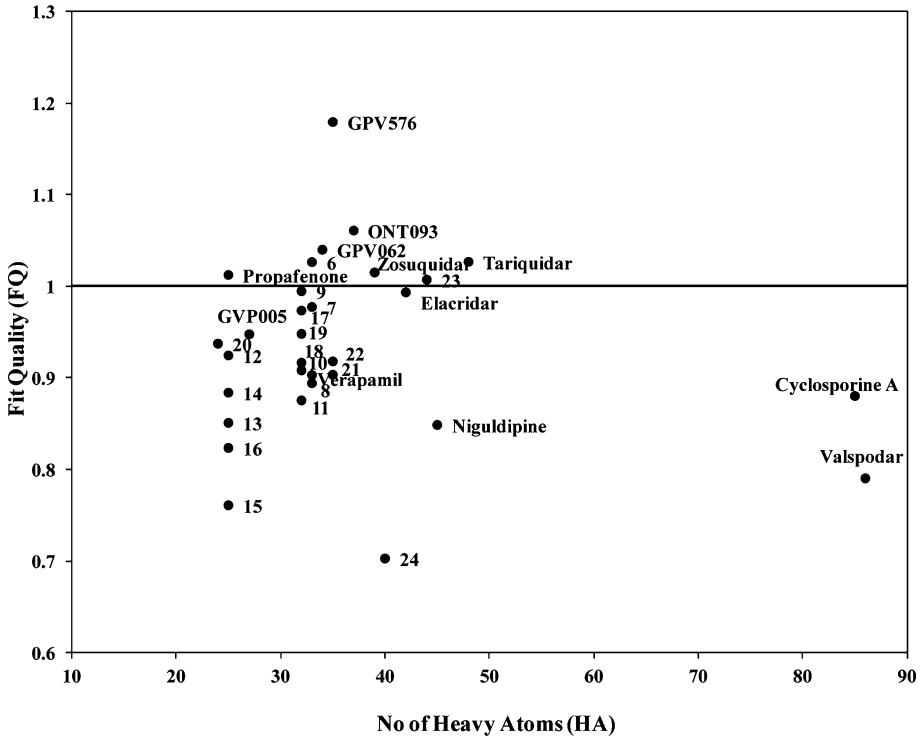


**Figure 4.** Fit quality scores vs heavy atom counts of benzophenones **6**–**24**, compounds which entered clinical studies, and selected propafenones. FQ score around **1** indicate a near optimal ligand binding affinity for a given number of heavy atoms.

**Table 2. Pharmacological Activities, Ligand Efficiency (LE), and Lipophilic Efficiency (LipE) Profiles of Selected Propafenones and P-gp Inhibitors Which Entered in Clinical Studies**

| compd | $pIC_{50}$ | HA | LE | clogP | LipE |
|---|---|---|---|---|---|
| Verapamil | 6.24 | 33 | 0.27 | 4.47 | 1.77 |
| Elacridar | 7.14 | 42 | 0.24 | 4.21 | 2.93 |
| Tariquidar | 7.48 | 48 | 0.22 | 5.55 | 1.93 |
| Zosuquidar | 7.23 | 39 | 0.26 | 4.96 | 2.27 |
| ONT093 | 7.50 | 37 | 0.29 | 7.30 | 0.19 |
| Valspodar | 6.30 | 86 | 0.10 | 15.09 | −8.79 |
| Cyclosporine A | 6.99 | 85 | 0.12 | 14.36 | −7.37 |
| Niguldipine | 6.15 | 45 | 0.20 | 7.80 | −1.65 |
| Propafenone | 6.48 | 25 | 0.37 | 3.64 | 2.84 |
| GPV576 | 8.25 | 35 | 0.33 | 6.02 | 2.23 |
| GPV062 | 7.24 | 34 | 0.30 | 4.15 | 3.09 |
| GPV005 | 6.22 | 27 | 0.33 | 4.38 | 1.84 |

benzophenones as well as for the compounds used for the LE study (Table 2). The clogP values vary from 2.66 to 15.09, leading to a lipophilic efficiency range between −8.79 and +3.08. This is somewhat surprising, as it has been reported that a lipophilic efficiency greater than 5 combined with clogP values between 2 and 3 is considered optimal for a promising drug candidate.[23,24] None of the clinically tested P-gp inhibitors fulfils these requirements. Only the 4-hydroxy-4-phenylpiperidine analogous propafenone GPV062 as well as the dimer **23** exhibit values slightly higher than 3. All other compounds show values lower than 3 (Figure 5). It is tempting to speculate whether this is due to the unique entrance pathway directly from the membrane bilayer, which requires a different logP profile than for compounds which access their binding site directly from the extracellular or intracellular aqueous compartment.

To study in more detail whether the unique access path of P-gp inhibitors directly from the membrane bilayer is linked to this unexpectedly low LipE values, we studied the distribution of LipE profiles for a set of targets showing different access pathways of their ligands: P-glycoprotein (via the membrane bilayer), the serotonin transporter SERT (from the extracellular environment), and the hERG potassium channel (from the cytoplasm) (Figure 6). LipE values of inhibitors of SERT (extracted from the ChemBL database),[40] hERG blockers,[41] and propafenone-type inhibitors of P-gp (in-house data) were calculated as described in the Materials and Methods section.

The LipE distribution profile of SERT inhibitors extracted from the ChemBL database identified about 13% of the compounds that cross the LipE threshold of 5 (Figure 7). These compounds cover a wide range of $IC_{50}$ (0.01 nM to 10 mM) and clogP (−3.42 to 4.66) (SM Figure 1). Moreover, 15 SERT inhibitors have been identified with clogP ∼ 2.5, LipE > 5, and $IC_{50}$ < 10 nM, none of them was listed as a marketed drug. In the case of hERG, only 2.5% of the compounds cross the LipE threshold of 5 that showed a potency distribution from 5 nM to 18 $\mu$M and clogP values between −0.77 and 2.21 (SM Figure 1). Only two compounds, almokalant and dofetilide, complied with the desired profile (clogP ∼ 2.5, LipE > 5, potency values <10 nM). Dofetilide is a registered class III antiarrhythmic agent, while almokalant is in phase II clinical investigations.[42,43]

LipE profiles of P-gp inhibitors could not identify any compound that reaches the standard threshold value of 5. Most of the ligands fall in the LipE range of 1–2 (39%) or 2–3 (28%), with wide a range in distribution of their clogP (0.40 to 6.02) as well as $IC_{50}$ (5.60 nM to 1.20 mM) values (SM Figure 1). Thus, the LipE threshold for ligands of P-gp needs to be reconsidered. Nevertheless, from the benzophenone data set presented here, compounds **16**, **19**, **20**, and **23** might be the


dx.doi.org/10.1021/jm201705f | J. Med. Chem. 2012, 55, 3261–3273

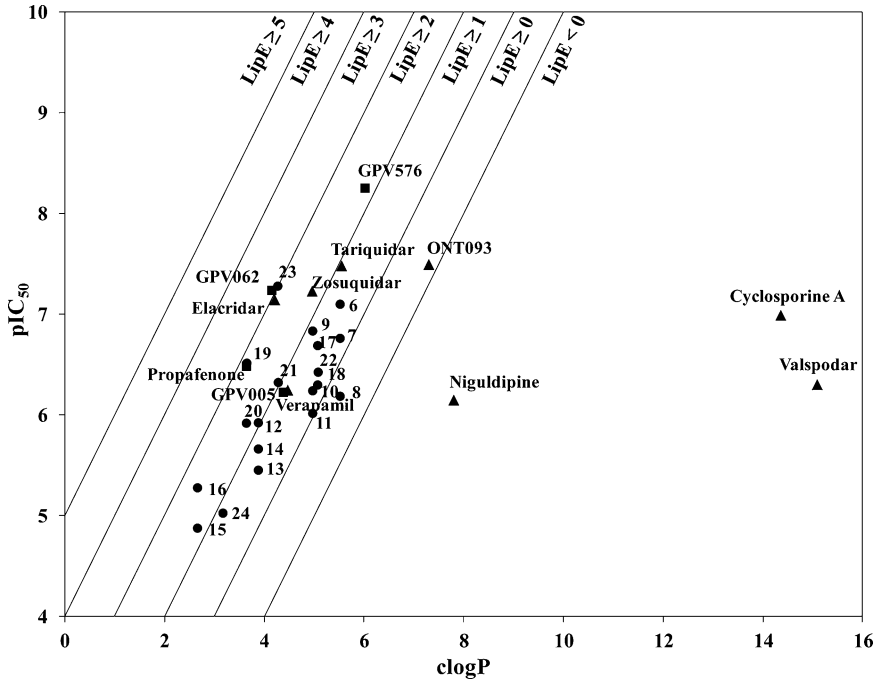


**Figure 5.** Plot of clogP vs biological activity of inhibitors of P-gp; LipE values higher than 5 are considered to be the threshold for compounds of clinical interest; ● benzophenones, ■ propafenones, ▲ compounds which entered clinical trials.

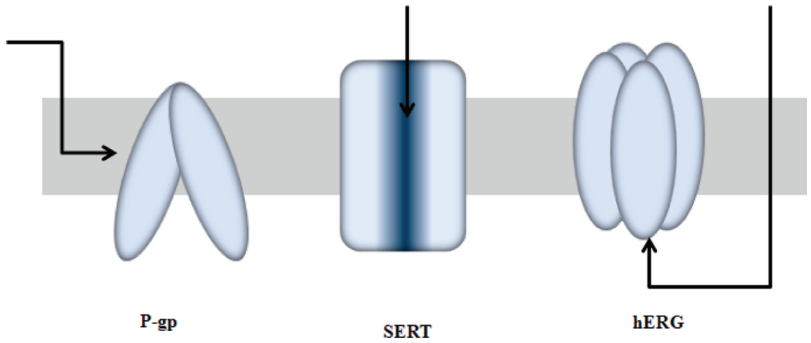


**Figure 6.** Schematic representation of access of inhibitors/substrates to the binding sites of P-gp, SERT, and hERG along three different pathways. Ligands of P-gp approach the binding cavity via the membrane bilayer; in SERT the ligands get access from the extracellular environment, while in hERG this access occurs via the cytoplasm.

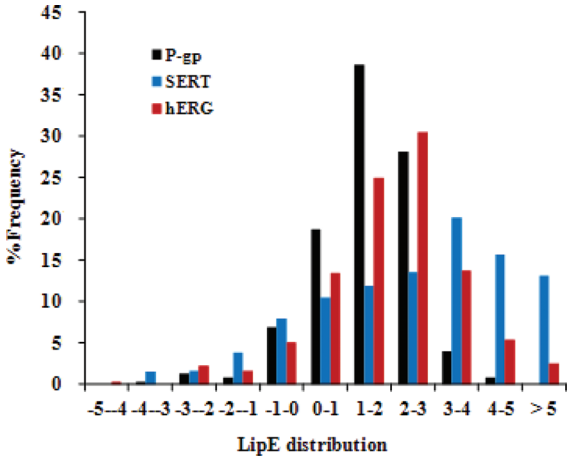


**Figure 7.** LipE distribution profiles of ligands of P-gp, SERT, and the hERG potassium channel.

most promising ones as their LipE values are between 2 and 3, a range where most of the compounds which in the past entered clinical trials are located.

**Docking into a Homology Model of P-Glycoprotein.** To get insights into the potential binding mode of propafenone-type benzophenones, we selected compounds **6**, **19**, and **20** and the dimer **23** for further in silico studies. Compounds **19**, **20**, and **23** were selected as they are ranked high both in LipE and FQ scores, and **6** was additionally included as it is top ranked with respect to FQ. Interestingly, this selection resembles the key features observed for propafenone analogues: compound **6** shows a 4-tolylpiperazine substituent (analogous to GPV576), compound **19** is analogous to GPV062 (4-hydroxy-4-phenyl-piperidine), and derivative **20** is the direct propafenone analogue (*N*-propyl). The docking protocol follows those previously published[44] and is provided in detail in the Materials and Methods section.

The analysis of the interaction pattern of selected docking poses indicates that the benzophenone scaffold interacts with F343 and F303 near the entry gate, whereas the lipophilic


dx.doi.org/10.1021/jm201705f | *J. Med. Chem.* 2012, 55, 3261–3273

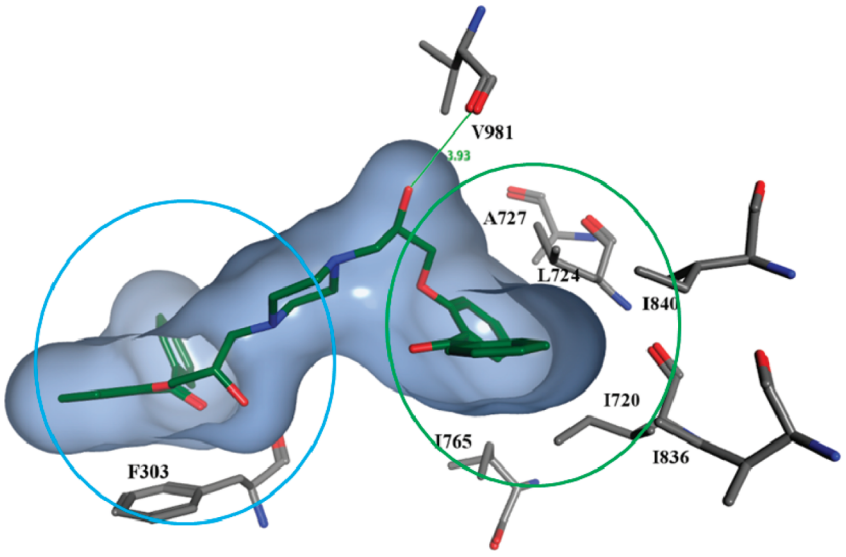


**Figure 8.** Ligand–protein interaction profile of the best scored pose of benzophenone dimer **23**. Blue circle represent the putative position of benzopyrano[3,4-*b*][1,4]oxazines having 4a*S*,10b*R* configuration, while the green circle indicates the position of diastereoisomers with 4a*R*,10b*S* configuration.

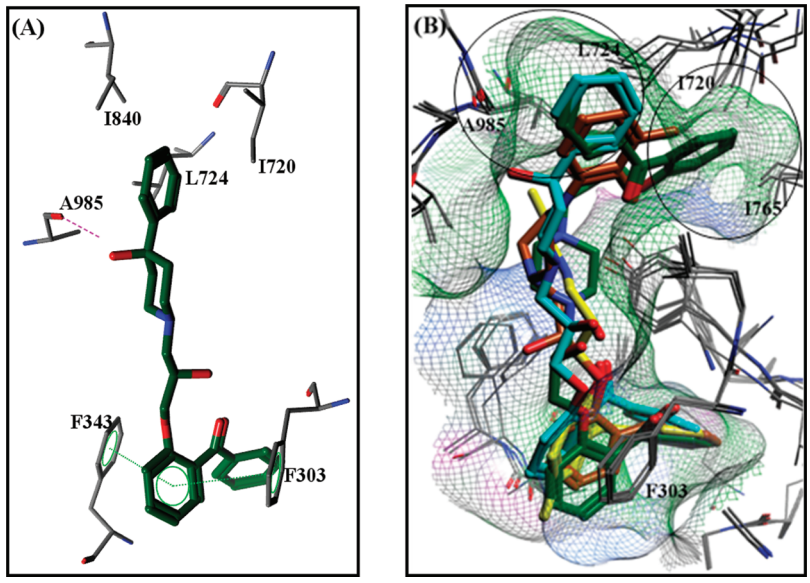


**Figure 9.** (A) Ligand protein interaction pattern of clustered pose of **19**. (B) Overlaid clustered poses (green, **23**; blue, **19**; yellow, **20**; brown, **6**). Two important hydrophobic binding cavities have been formed by amino acid residues of TM 7, 8, 9, and 12, indicated by two circles.

substituents in the vicinity of the basic nitrogen atom are surrounded by hydrophobic amino acid residues L724, I720, V981, I840, I836, and I765 located at TM 7, 8, 9, and 12 (Figure 8). This further supports the importance of high lipophilicity and also is in line with previous studies performed by Pajeva and Wiese, who showed that for a series of inhibitors of P-gp hydrophobicity represents a space directed molecular property rather than a simple overall descriptor.[45] The top ranked cluster of poses are in close vicinity of our previously purposed binding positions for benzopyrano[3,4-*b*][1,4]-oxazines, where compounds having 4a*S*,10b*R* configuration interact mainly with amino acid residues of TM 4, 5, and 6 near the entry gate, while compounds having 4a*R*,10b*S* configuration are positioned deeper inside the binding cavity, being mainly surrounded by hydrophobic amino acid residues of TM 7, 8, 9, and 12.[44] Interestingly, the top scored dimer **23** is positioned in a way to bridge these two positions (Figure 8). Moreover, this pose might also aid in the explanation for the activity differences of homodimer **23** (0.05 $\mu$M) and heterodimer **22** (9.48 $\mu$M): The additional benzene ring in the best scored pose of homodimer **23** is surrounded by several hydrophobic amino acids (I836, L720, I840, and L724).

A representative docking pose of the 4-hydroxy-4-phenyl-piperidine derivative **19** showed an H-bond interaction between the 4-hydroxy group and A985 (Figure 9A). This further supports our SAR data and strengthens the importance of 4-hydroxy-4-phenyl-piperidine moieties for high inhibitory potency of propafenones and benzophenones. Furthermore, A985 was also identified as interacting with verapamil and the cyclic peptide (AQZ59-SSS) cocrystallized in mouse P-gp.[19] A binding pocket of 4.5 Å around interacting amino acid residues of TM 7, 8, 9, and 12 showed two small hydrophobic cavities


dx.doi.org/10.1021/jm201705f | *J. Med. Chem.* 2012, 55, 3261–3273

(encircled in Figure 9B), occupying the hydrophobic substituents at the basic nitrogen atom of the ligands. A closer look of the overlaid poses shows that the benzophenone substituent in dimer **23** fits well in the hydrophobic pockets, which might explain its high FQ score.

Overall, benzophenones shared a similar interaction profile as propafenones. Amino acids S952, F434, F336, L724, and Y307 have been identified as common interacting amino acid residues of all three classes of propafenone type inhibitors of P-gp (SM Figure 3). Selected benzophenone analogues have been previously used as photoaffinity ligands to characterize the drug-binding domain of propafenone-type analogues. In these studies, TM 3, 5, 6, 8, 10, 11, and 12 were identified as potential interacting helices.[30,46,47] This is well in line with our docking studies, which show main interactions with TM 5 and 6 near the entry gate and TM 7, 8, 9, and 12 deeper inside the cavity (SM Figure 4). No significant cluster of poses has been identified on the second wing (2/11 interface), which might be due to the asymmetry in the template used for building the homology model of P-gp, thus narrowing the available space at this side.

## CONCLUSIONS

Calculation of ligand efficiency and lipophilic efficiency values for a set of P-gp inhibitors shows that ligands of P-gp exhibit LipE values below the threshold of 5 considered to be optimal for clinical candidates. This might be due to the unique entrance pathway of these classes of compounds, taking a route directly from the membrane bilayer. However, LipE and LE values of benzophenones **6**, **19**, and **20**, as well as of the dimer **23**, are close to compounds which entered clinical studies, thus qualifying them for further lead optimization cycles. Docking studies further strengthen the evidence provided by QSAR studies that the benzophenones bind to the same region as propafenone-type inhibitors. Moreover, the dimer **23** seems to bridge the two distinct binding sites recently proposed for benzopyrano[3,4-*b*][1,4]oxazines. This further supports the general assumption of a binding zone with distinct, but overlapping binding sites for individual scaffolds as a basis for the promiscuity of P-gp.

## EXPERIMENTAL SECTION

**Chemistry.** *Material and Methods.* The data set used consists of a set of previously published benzophenones **9**[37] and **12**, **19**, and **20**[29] as well as a series of newly synthesized analogues. Melting points were determined on Leica Galen III (ser. no. 1413 WT) and are uncorrected. Purity of the compounds was checked by elemental analysis, and all values were within ±0.3%. Elemental analysis was performed at Microanalytical Laboratory of the Institute of Physical Chemistry (Mag. Johannes Theiner), University of Vienna. The equipment used was a 2400 CHN-Elemental Analyzer from Perkin-Elmer. Mass spectra were recorded on a Maldi-TOF, Kratos Instruments, matrix assisted laser-desorption-ionization time-of-flight, reflection mass spectrometer. NMR spectra were recorded on a Bruker spectrospin for 200 MHz $^1$H NMR and 50 MHz for $^{13}$C NMR. $CDCl_3$ and DMSO at room temperature were used as internal standards. Column chromatographic separations were performed by using silica gel 60 (Particle size 40−63 μm, 230−300 mesh) from J. T. Baker or Merck. Thin layer chromatography (TLC) was performed on silica gel 60F254 TLC plates from Merck.

*General Procedure for the Preparation of (2-Oxiranylmethoxy-phenyl)-phenyl-methanone $C_{16}H_{14}O_3$ (**2a**).* First, 10 g (51 mmol) of 2-hydroxy-benzophenone was dissolved in epichlorohydrine (120 mL), treated with 2.04 g (51 mmol) of sodium hydroxide, and refluxed for 24 h. Then, after cooling, the residue was filtered off and washed with diethyl ether. Subsequently, the solvent was removed by rotary evaporation. The remaining oil was taken up in diethyl ether and washed with water (175 mL). The organic phase was then dried over anhydrous sodium sulfate. After removal of the solvent by rotary evaporation, yellow oil was obtained, yield 12.81 g (98.85%). $^1$H NMR ($CDCl_3$) $\delta$ 2.37−2.66 (m, 2H, $CH_2$-O-CH), 2.96−3.00 (m, 1H, CH), 3.92−4.15 (m, 2H, Ar-O-$CH_2$), 6.97−7.81 (m, 9H, arom H). $^{13}$C NMR ($CDCl_3$) $\delta$ 44.03 (CH-$CH_2$-O), 49.59 (CH), 68.62 (Ar-O-$CH_2$), 112.72, 121.13, 128.05 (arom C), 129.00 (Ar-CO), 129.38, 129.69, 131.97, 132.66 (arom C), 137.93 (Ph-CO), 156.08 (Ar-O), 196.15 (CO).

*General Procedure for the Preparation of (3-Oxiranylmethoxy-phenyl)-phenyl-methanone $C_{16}H_{14}O_3$ (**2b**).* First, 5 g (25.25 mmol) of 3-hydroxy-benzophenone was dissolved in epichlorohydrine (60 mL), treated with 1.01 g (25.25 mmol) of sodium hydroxide, refluxed for 6 h, and stirred overnight. Then the residue was filtered off and washed with diethyl ether. After removal of the solvents under reduced pressure, the resulting oil was taken up in diethyl ether and washed with water several times. The organic layers were combined, dried over anhydrous sodium sulfate, and evaporated to dryness yielding yellow oil. For further purification a column chromatography (silica gel, ether/petrol ether, 70 + 30) was performed. Subsequent removal of the solvents under reduced pressure gave white opalescent oil, yield 6 g (93.6%). $^1$H NMR ($CDCl_3$) $\delta$ 2.71−2.74 (m, 1H, $H_A$), 2.86 (t, 1H, $J$ = 4.42, $H_B$), 3.29−3.37 (m, 1H, CH), 3.93 (dd, 1H, $J$ = 5.94/11.12, $H_X$), 4.28 (dd, H, $J$ = 2.90/10.98, $H_Y$), 7.10−7.78 (arom H). $^{13}$C NMR ($CDCl_3$) $\delta$ 44.34 ($CH_2$−O), 49.81 (CH), 68.76 (Ar-O-$CH_2$), 114.93, 119.17, 123.10, 128.11, 129.18, 129.81, 132.31, (arom C), 137.28, 138.70 (C), 158.24 (Ar-O), 196.08 (CO).

*General Procedure for the Preparation of (4-Oxiranylmethoxy-phenyl)-phenyl-methanone $C_{16}H_{14}O_3$ (**2c**).* first, 6 g (30.30 mmol) of 4-hydroxy-benzophenone was dissolved in epichlorohydrine (50 mL), treated with 2 g (50 mmol) of sodium hydroxide, refluxed for 5 h, and stirred overnight. The residue was filtered off and washed with diethyl ether. Subsequently, the solvent was removed by rotary evaporation. The remaining opalescent oil was taken up in diethyl ether and washed with water several times. The organic phase was then dried over anhydrous sodium sulfate. After removal of the solvents by rotary evaporation, a white solid was obtained, yield 6.7 g (87.54%). $^1$H NMR ($CDCl_3$) $\delta$ 2.76 (dd, 1H, $J$ = 2.66/4.8, $H_A$), 2.92 (t, 1H, $J$ = 4.64, $H_B$), 3.35−3.40 (m, 1H, CH), 3.96−4.0 (dd, 1H, $J$ = 5.81−11.12, $H_X$), 4.29−4.36 (dd, 1H, $J$ = 2.91/11.11, $H_Y$), 6.95−7.00 (m, 2H, H-3, H-5), 7.42−7.56 (m, 5H, H-2, H-6, H-3′, H-4′, H-5′), 7.72−7.83 (m, 2H, H-2′, H-6′). $^{13}$C NMR ($CDCl_3$) $\delta$ 44.51 ($CH_2$-O), 49.84 (CH), 68.82 (Ar-O-$CH_2$), 114.07, 128.14, 129.65, 131.90, 132.46, (arom C), 130.54 (Ar-CO), 138.06 (Ph-CO), 161.93 (Ar-O), 195.41 (CO).

*General Procedure for the Preparation of [2-(2-Hydroxy-3-piperazine-1-yl-propoxy)-phenyl]-phenyl-methanone (**5**).* First, 1.82 g (7.20 mmol) of (2-oxiranylmethoxy-phenyl)-phenyl-methanone (**2a**) was dissolved in 20−30 mL of methanol, 1.6 g (18.6 mmol) of piperazine was added, and then the reaction mixture was refluxed for 5 h. After removal of the solvent by rotary evaporation, a column chromatography was performed (silica gel, $CH_2Cl_2$/methanol/concentrated $NH_3$, 100/10/1) subsequent evaporation to dryness yielded 1.88 g (77.33%) of yellow oil which was solidified on cooling. $^1$H NMR ($CDCl_3$) $\delta$ 2.01−2.42 (m, 6H, $CH_2$-N-($CH_2$)$_2$), 2.77−2.81 (m, 4H, ($CH_2$)$_2$-N), 3.68−3.75 (m, 1H, CH), 3.90−3.94 (m, 2H, O−$CH_2$), 6.96−7.79 (m, 9H, arom H). $^{13}$C NMR ($CDCl_3$) $\delta$ 45.86 (N-($CH_2$)$_2$), 54.30 (($CH_2$)$_2$-NH), 60.79 ($CH_2$-N), 65.27 (CH), 70.76 (O-$CH_2$), 112.56, 121.05, 128.28, 129.51, 130.07, 132.33, 132.83 (arom C), 128.79 (Ar-CO), 138.36 (Ph-CO), 156.55 (arom C-O), 196.56 (CO).

*(2-{3-[4-(2,3-Xylyl)-piperazine-1-yl]-2-hydroxy-propoxy}-phenyl)-phenyl-methanone (**6**).* First, 700 mg (2.75 mmol) of (2-oxiranylmethoxy-phenyl)-phenyl-methanone (**2a**) was dissolved in 15 mL of methanol and treated with 526 mg (2.75 mmol) of 1-(2,3-xylyl)-piperazine. The mixture was refluxed for 24 h. Subsequent removal of the solvent yielded yellow oil, crystallization from ethyl

acetate/diethylether gave 904 mg (73.8%) white crystals; mp 116−118 °C. $^1$H NMR ($CDCl_3$) $\delta$ 2.19−2.27 (m, 2H, $CH_2$), 2.21 (s, 3H, $CH_3$), 2.27 (s, 3H, $CH_3$), 2.42−2.47 (m, 2H, $CH_2$), 2.58−2.66 (m, 2H, $CH_2$), 2.83−2.88 (m, 4H, $(CH_2)_2$-*N*-Xyl), 3.77−3.83 (m, 1H, CH), 3.91−4.02 (m, 2H, O-$CH_2$), 6.90 (dd, 2H, $J$ = 2.90/7.83 Hz, arom H), 6.99−7.12 (m, 3H, arom H), 7.44−7.58 (m, 5H, arom H), 7.79−7.83 (m, 2H, arom H). $^{13}$C NMR ($CDCl_3$) $\delta$ 13.93 ($CH_3$-*ortho*), 20.61 ($CH_3$-*meta*), 51.97 (*N*-$(CH_2)_2$), 53.79 ($CH_2$-N), 60.36 (($CH_2)_2$-*N*-Ph), 65.42 (CH), 70.75 (O-$CH_2$), 112.64, 116.56, 121.12, 125.01, 125.81, 128.33, 128.86, 129.58, 130.12, 132.37, 132.87 (arom C), 137.99 (Ar-CO), 138.43 (Ph-CO), 151.29 (Ar-N), 156.58 (Ar-O). MS $m/e$ 556.25 ($M^+$, 100%). Anal. Calcd for $C_{28}H_{32}N_2O_3$: C, 74.89; H, 7.29; N, 6.24. Found: C, 74.73; H, 7.59; N, 6.32.

*(3-{3-[4-(2,3-Xylyl)-piperazine-1-yl]-2-hydroxy-propoxy}-phenyl)-phenyl-methanone (**7**).* First, 560 mg (2.20 mmol) of 3-oxiranylmethoxy-phenyl)-phenyl-methanone (**2b**) was dissolved in 20 mL of methanol and treated with 418 mg (2.20 mmol) of 1-(2,3-xylyl)-piperazine. Then the mixture was refluxed for 6 h. After removal of the solvent under reduced pressure, a yellow oil was obtained which was crystallized from ethyl acetate/diethyl ether, yielding 960 mg (98%) white crystals; mp 92−99 °C. $^1$H NMR ($CDCl_3$) $\delta$ 2.23, 2.27 (2s, 6H, 2$CH_3$), 2.62−2.66 (m, 4H, *N*-$(CH_2)_2$), 2.83−2.93 (m, 6H, $CH_2$-N, $(CH_2)_2$-*N*-Ph), 4.08−4.18 (m, 3H, O-$CH_2$-CH), 6.92 (d, 2H, $J$ = 7.07, H-4, H-6), 7.05−7.20 (m, 2H, arom H), 7.37−7.79 (m, 6H, arom H), 7.80−7.83 (m, 2H, arom H). $^{13}$C NMR ($CDCl_3$) $\delta$ 13.92 ($CH_3$-*ortho*), 20.60 ($CH_3$-*meta*), 52.15 (*N*-$(CH_2)_2$), 53.77 (($CH_2)_2$-N), 60.38 ($CH_2$-N), 65.38(CH), 70.49(O-$CH_2$), 115.07, 116.58, 119.30, 123.09, 125.03, 125.81, 128.24, 129.26, 130.00 (arom C), 131.19 (C), 132.42 (arom C), 137.52, 137.97, 138.86, 151.31 (C), 158.70 (Ar-O), 196.41(CO). MS $m/e$ 444.68 (M, 90%). Anal. Calcd for $C_{28}H_{32}N_2O_3 \cdot 0.3H_2O$: C, 74.64; H, 7.31; N, 6.22. Found: C, 74.76; H, 7.56; N, 6.08.

*(4-{3-[4-(2,3-Xylyl)-piperazine-1-yl]-2-hydroxy-propoxy}-phenyl)-phenyl-methanone (**8**).* First, 700 mg (2.76 mmol) of (4-oxiranylmethoxy-phenyl)-phenyl-methanone (**2c**) was dissolved in 15 mL of methanol, treated with 523.6 mg (2.756 mmol) of 1-(2,3 xylyl)-piperazine, and the mixture was refluxed for 5 h. Then, removal of the solvent under reduced pressure yielded white crystals which were recrystallized from methanol giving 1.06 g (94.62%) white crystals; mp 122−126 °C. $^1$H NMR ($CDCl_3$) $\delta$ 2.23−2.27 (2s, 6H, 2$CH_3$), 2.55−2.70 (m, 4H, $(CH_2)_2$-*N*-Ph), 2.70−3.00 (m, 6H, $CH_2$-N-$(CH_2)_2$), 3.40−3.70 (bs, 1H, OH), 4.10−4.17 (m, 3H, O-$CH_2$-CH), 6.90−7.03 (m, 5H, arom H), 7.44−7.51 (m, 3H, arom H), 7.74−7.81 (m, 4H, arom H). $^{13}$C NMR ($CDCl_3$) $\delta$ 13.90 ($CH_3$-*ortho*), 20.58 ($CH_3$-*meta*), 52.15, 53.76 ($CH_2$-N-$(CH_2)_2$), 60.38 (($CH_2)_2$-N), 65.31 (CH), 70.44 (O-$CH_2$), 114.08, 116.57, 125.05, 125.81, 128.15, 129.69 (arom C), 130.37, 131.88 (C), 131.88, 132.50 (arom C), 137.97, 138.18 (C), 151.29 (Ar-N), 162.34 (Ar-O), 195.50 (CO). MS $m/e$ 445.4 ($M^+$, 100%). Anal. Calcd for $C_{28}H_{32}N_2O_3$: C, 75.65; H, 7.26; N, 6.30. Found: C, 75.61; H, 7.48; N, 6.33.

*(3-{3-[4-(4-Fluoro-phenyl)-piperazine-1-yl]-2hydroxy-propoxy}-phenyl)-phenyl-methanone (**10**).* First, 500 mg (1.97 mmol) of (3-oxiranylmethoxy-phenyl)-phenyl-methanone (**2b**) was dissolved in 15 mL of methanol, treated with 360 mg (2 mmol) of *p*-F-phenyl-piperazine, and the mixture was refluxed for 6 h. Then the solution was allowed to cool down and stirred at room temperature overnight. The obtained solid was filtered off and washed with diethyl ether, giving 690 mg (80.76%) white crystals; mp 131−133 °C. $^1$H NMR ($CDCl_3$) $\delta$ 2.60−2.85 (m, 6H, $CH_2$-N-$(CH_2)_2$), 3.12−3.17 (m, 4H, $(CH_2)_2$-*N*-Ph), 4.05−4.18 (m, 3H, O-$CH_2$-CH-OH), 6.87−6.97 (m, 4H, arom H), 7.19−7.25 (m, 1H, arom H), 7.37−7.60 (m, 6H, arom H), 7.78−7.82 (m, 2H, arom H). $^{13}$C NMR ($CDCl_3$) $\delta$ 50.18, 53.28, 60.30 ($CH_2$-N-$(CH_2)_4$), 65.46 (CH), 70.36 (O-$CH_2$), 115.04, 115.29, 115.73, 117.81, 117.97, 119.28, 123.15, 128.24, 129.99, 132.43 (arom C), 137.48 (Ar-CO), 138.87 (Ph-CO), 147.71 (Ar-N), 157.22 ($J$ = 239 Hz, C-F), 158.64 (Ar-O), 196.39 (CO). MS $m/e$ 434.77 (M, 100%). Anal. Calcd for $C_{26}H_{27}FN_2O_3$: C, 71.87; H, 6.26; N,6.45. Found: C, 71.65; H, 6.45; N, 6.46.

*(4-{3-[4-(4-Fluoro-phenyl)-piperazine-1-yl]-2-hydroxy-propoxy}-phenyl)-phenyl-methanone (**11**).* First, 700 mg (2.75 mmol) of (4-oxiranylmethoxy-phenyl)-phenyl-methanone (**2c**) was dissolved in 15 mL of methanol, treated with 496 mg (2.75 mmol) of *p*-F-phenyl-piperazine, and refluxed for 5 h. Then removal of solvent under reduced pressure left a yellow oil which was crystallized from isopropyl alcohol, yielding 1 g (83.6%) white crystals; mp 96−100 °C. $^1$H NMR ($CDCl_3$) $\delta$ 2.61−2.69 (m, 4H, N-$(CH_2)_2$), 2.80−2.91 (m, 2H, $CH_2$-N), 3.12−3.17 (m, 4H, $(CH_2)_2$-*N*-Ph), 3.56 (br, 1H, OH), 4.11−4.19 (m, 3H, $CH_2$-CH), 6.89−7.85 (m, 13H, arom H). $^{13}$C NMR ($CDCl_3$) $\delta$ 50.24, 53.28, 60.28 ($CH_2$-N-$(CH_2)_4$), 65.40 (CH), 70.33 (O-$CH_2$), 114.07, 115.31, 115.75, 117.81, 117.96, 128.17, 129.71, (arom C), 130.42 (Ar-CO), 131.92, 132.52 (arom C), 138.15 (Ph-CO), 147.77 (Ar-N), 162.28 (Ar-O), 195.50 (CO). MS $m/e$ 435.3 ($M^+$, 100%). Anal. Calcd for $C_{26}H_{27}FN_2O_3$: C, 71.87; H, 6.26; N, 6.45. Found: C, 71.61; H, 6.43; N, 6.41.

*[3-(2-Hydroxy-3-piperidine-1-yl-propoxy)-phenyl]-phenyl-methanone (**13**).* First, 700 mg (2.75 mmol) of (3-oxiranylmethoxy-phenyl)-phenyl-methanone (**2b**) was dissolved in 15 mL of methanol and treated with 234 mg (2.75 mmol) of piperidine. Then the mixture was refluxed for 4 h and stirred at room temperature overnight. After removal of the solvent under reduced pressure, 336 mg (36%) yellow oil was obtained; mp 64 °C. $^1$H NMR ($CDCl_3$) $\delta$ 1.45−1.59 (m, 6H, $CH_2$), 2.37−2.50 (m, 4H, N-$(CH_2)_2$), 2.56−2.62 (m, 2H, $CH_2$-N), 4.02−4.13 (m, 3H, O-$CH_2$-CH), 7.13−7.81 (m, 9H, arom H). $^{13}$C NMR ($CDCl_3$) $\delta$ 24.17, 26.05 ($CH_2$), 54.67 (*N*-$(CH_2)_2$), 60.89 ($CH_2$-N), 65.18 (CH), 70.64 (O-$CH_2$), 115.11, 119.28, 122.99, 128.23, 129.22 130.00, 132.39 (arom C), 137.54, 138.82 (C), 158.75 (Ar-O), 196.44 (CO). MS $m/e$ 340.43 ($M^+$, 100%). Anal. Calcd for $C_{21}H_{25}NO_3$: C, 73.53; H, 7.46; N, 4.08. Found: C, 73.51; H, 7.71; N, 4.11.

*[4-(2-Hydroxy-3-piperidine-1-yl-propoxy)-phenyl]-phenyl-methanone (**14**).* First, 700 mg (2.75 mmol) of (4-oxiranylmethoxy-phenyl)-phenyl-methanone (**2c**) was dissolved in 10 mL of piperidine and refluxed for 2.5 h. Then after removal of piperidine under reduced pressure, a yellow oil was obtained. For further purification, a column chromatography was performed (silica gel, $CH_2Cl_2$/methanol/concentrated $NH_3$, 95/5/1 after removal of piperidine the percentage of methanol was increased to 80/20/1). Solvents were removed by rotary evaporation to yield light-yellow oil, which crystallized from ethyl acetate. Further recrystallization from methanol/diethyl ether yielded 400 mg (42.8%) white crystals; mp 106 °C. $^1$H NMR ($CDCl_3$) $\delta$ 1.49−1.72 (m, 6H, $CH_2$), 2.58−2.73 (m, 6H, $CH_2$-N-$(CH_2)_2$), 4.05−4.08 (m, 2H, O-$CH_2$), 4.20−4.29 (m, 1H, CH), 4.32 (s, 1H, OH), 6.97 (d, 2H, $J$ = 8.85, H-3, H-5), 7.45−7.82 (m, 7H, arom H). $^{13}$C NMR ($CDCl_3$) $\delta$ 23.65, 25.33 ($CH_2$), 54.78 (*N*-$(CH_2)_2$), 61.21 ($CH_2$-N), 64.89 (CH), 70.64 (O-$CH_2$), 114.06, 128.15, 129.67 (arom $C_r$), 130.38 (Ar-O), 131.89, 132.48 (arom C), 138.13 (Ph-CO), 162.21 (Ar-O), 195.49 (CO). MS $m/e$ 340.3 ($M^+$, 100%). Anal. Calcd for $C_{21}H_{25}NO_3$: C, 71.77; H, 7.55; N, 3.99. Found: C, 71.68; H, 7.51; N, 4.02.

*[2-(2-Hydroxy-3-morpholine-4-yl-propoxy)-phenyl]-phenyl-methanone (**15**).* First, 1 g (4.33 mmol) of (2-oxiranylmethoxy-phenyl)-phenyl-methanone (**2a**) was dissolved in 20 mL of methanol and treated with 500 mg (5.75 mmol) of morpholine. Then the mixture was refluxed for 4 h. Removal of the solvents gives yellow oil, which was purified via column chromatography (silica gel, $CH_2Cl_2$/methanol/concentrated $NH_3$, 200/10/1). Subsequent removal of the solvents under reduced pressure yielded 400 mg (27%) of light-yellow oil; mp 185−193 °C. $^1$H NMR ($CDCl_3$) $\delta$ 1.97−2.46 (m, 6H, $CH_2$-N-$(CH_2)_2$), 3.73 (t, 2H, $J$ = 4.67, O-$CH_2$), 3.71−3.80 (m, 4H, O-$(CH_2)_2$), 6.95−7.10 (m, 2H, arom H), 7.41−7.58 (m, 5H, arom H), 7.75−7.79 (m, 5H, arom H). $^{13}$C NMR ($CDCl_3$) $\delta$ 53.57, 60.68 ($CH_2$-N-$(CH_2)_2$), 62.24 (CH), 66.68 (O-$(CH_2)_2$), 70.60 (O-$CH_3$), 112.54, 121.07, 128.25 (arom C), 128.72 (Ar-CO), 129.48, 130.04, 132.31, 132.80 (arom C), 138.31 (Ph-CO), 156.45 (Ar-O), 196.41 (CO). MS $m/e$ 341.50 (M, 20%). Anal. Calcd for $C_{20}H_{23}NO_4$: C, 68.55; H, 6.90; N, 4.00. Found: C, 68.30; H, 6.62; N, 4.29.

*[4-(2-Hydroxy-3-morpholine-4-yl-propoxy)-phenyl]-phenyl-methanone (**16**).* First, 700 mg (2.75 mmol) of (4-oxiranylmethoxy-phenyl)-phenyl-methanone (**2c**) was dissolved in 15 mL of methanol, treated with 240 mg of morpholine, and refluxed for 7 h. Then

subsequent removal of the solvent under reduced pressure left 910 mg (96.8%) of yellow oil; mp 135−141 °C. $^1$H NMR ($CDCl_3$) $\delta$ 2.44−2.71 (m, 6H, $CH_2$-N-$(CH_2)_2$), 3.73 (t, 4H, $J$ = 4.56, $(CH_2)_2$-O), 4.06−4.17 (m, 3H, O-$CH_2$), 6.98 (d, 2H, $J$ = 8.82, H-3, H-5), 7.42−7.56 (m, 3H, arom H), 7.72−7.84 (m, 4H, arom H). $^{13}$C NMR ($CDCl_3$) $\delta$ 53.69, 60.83 ($CH_2$-N-$(CH_2)_2$), 65.18 (CH), 66.94 ($(CH_2)_2$-O), 70.28 (O-$CH_2$), 114.04, 128.15, 129.68 (arom C), 130.40 (Ar-CO), 131.90, 132.49 (arom C), 138.13 (Ph-CO), 162.24 (Ar-O), 195.48 (CO). MS $m/e$ 342.30 ($M^+$, 95%). Anal. Calcd for $C_{20}H_{23}NO_4$: C, 69.15; H, 6.87; N, 4.03. Found: C, 69.16; H, 7.07; N, 4.18.

*{3-[2-Hydroxy-3-(4-o-tolyl-piperazine-1-yl)-propoxy]-phenyl}-phenyl-methanone (**17**).* First, 700 mg (2.75 mmol) of (3-oxiranylmethoxy-phenyl)-phenyl-methanone (**2b**) was dissolved in 15 mL of methanol and treated with 500 mg (2.84 mmol) of *o*-tolyl-piperazine, and the mixture was refluxed for 6 h. Then subsequent removal of the solvent yielded 1.07 g (90.29%) of yellow oil; mp 173−179 °C. $^1$H NMR ($CDCl_3$) $\delta$ 2.31 (s, 3H, $CH_3$), 2.61−2.66 (m, 4H, N$(CH_2)_2$), 2.28−2.96 (m, 6H, $CH_2$-N, $(CH_2)_2$)-*N*-Phe), 4.05−4.18 (m, 3H, O-$CH_2$-CH), 6.99−7.05 (m, 2H, arom H), 7.37−7.60 (m, 6H, arom H), 7.79−7.83 (m, 2H, arom H). $^{13}$C NMR ($CDCl_3$) $\delta$ 17.82 ($CH_3$), 51.71 (*N*-$(CH_2)_2$), 53.74 ($CH_2$-N), 60.34 ($(CH_2)_2$-*N*-Ph), 65.37(CH), 70.46 (O-$CH_2$), 115.05, 118.92, 119.28, 123.07, 123.18, 126.53, 128.23, 129.23, 131.02, 132.40 (arom C), 132.40 (Ar-CO), 138.83 (Ph-CO), 151.23 (Ar−N), 158.68 (Ar-O), 196.40 (CO). MS $m/e$ 430.52 (M, 20%). Anal. Calcd for $C_{27}H_{30}N_2O_3$: C, 73.78; H, 7.11; N, 6.37. Found. C, 73.71; H, 7.31; N, 6.24.

*{4-[2-Hydroxy-3-(4-o-tolyl-piperazine-1-yl)-propoxy]-phenyl}-phenyl-methanone (**18**).* First, 700 mg (2.75 mmol) of (4-oxiranylmethoxy-phenyl)-phenyl-methanone (**2c**) was dissolved in 15 mL of methanol and treated with 500 mg (2.84 mmol) of *o*-tolyl-piperazine, and the mixture was refluxed for 5 h. Then subsequent removal of the solvent under reduced pressure yield 1.1 g (92.83%) of white crystals, which were recrystallized from methanol; mp 107−114 °C. $^1$H NMR ($CDCl_3$) $\delta$ 2.31 (s, 3H, $CH_3$), 2.63−2.67 (m, 4H, N$(CH_2)_2$), 2.84−2.97 (m, 6H, $CH_2$-N, $(CH_2)_2$)-*N*-Ph), 4.10−4.22 (m, 3H, O-$CH_2$-CH), 6.99−7.03 (m, 4H, arom H), 7.15−7.21 (m, 2H, arom H), 7.48−7.58 (m, 3H, arom H), 7.74−7.86 (m, 4H, arom H). $^{13}$C NMR ($CDCl_3$) $\delta$ 17.82 ($CH_3$), 51.74 (*N*-$(CH_2)_2$), 53.74 ($CH_2$-N), 60.36 ($(CH_2)_2$-*N*-Ph), 65.29 (CH), 70.42 (O-$CH_2$), 114.09, 118.94, 123.24, 126.57, 128.17, 129.71, (arom C), 130.38 (Ar-CO), 131.06, 131.90, 132.52 (arom C), 138.18 (Ph-CO), 151.22 (Ar-N), 162.34 (Ar-O), 195.51 (CO); MS $m/e$ 431.4 ($M^+$, 100%). Anal. Calcd for $C_{27}H_{30}N_2O_3$: C, 75.32; H, 7.02; N, 6.51. Found: C, 75.11; H, 7.12; N, 6.39.

*4-[3-(2-Benzoyl-phenoxy)-2-hydroxy-propyl]-piperazine-1-carboxylic Acid p-Tolylamide (**21**).* First, 186 mg (0.54 mmol) of [2-(2-hydroxy-3-piperazine-1-yl-propoxy)-phenyl]-phenyl-methanone (**5**) was dissolved in 15 mL of dichloromethane, and then a solution of 75 mg (0.57 mmol) of 4-methyl phenyl isocyanate in dichloromethane was added dropwise. The mixture was stirred at room temperature and monitored by TLC. After evaporation to dryness, a yellow oil was obtained which was purified by column chromatography (silica gel, $CH_2Cl_2$/methanol/concentrated $NH_3$, 100/10/1). Subsequent removal of the solvents under reduced pressure yielded 136 mg (52.56%) of a colorless oil. $^1$H NMR ($CDCl_3$) $\delta$ 2.41−2.53 (m, 6H, $CH_2$-N-$(CH_2)_2$), 2.43 (s, 3H, $CH_3$), 3.13 (s, 1H, OH), 3.51−3.53 (m, 4H, $(CH_2)_2$-N), 3.86−3.95 (m, 1H, CH), 4.09 (d, 2H, $J$ = 4.80, O-$CH_2$), 7.08−7.96 (m, 14H, arom H, NH). $^{13}$C NMR ($CDCl_3$) $\delta$ 20.57 ($CH_3$), 43.70 ($(CH_2)_2$-N-CO), 52.76 (*N*-$(CH_2)_2$), 59.97 ($CH_2$-N), 65.60 (CH), 70.60 (O-$CH_2$), 112.56, 120.32, 120.96, 128.20, 29.07, 129.42, 129.88, 132.27, 132.85 (arom C), 128.54 (Ar-CO), 132.30 (Ar-$CH_3$), 136.38 (NH-Ar), 138.08 (Ph-CO), 155.24 (N-CO-NH), 156.39 (arom C−O), 196.54 (CO). MS $m/e$ 473.8 (M, 18%). Anal. Calcd for $C_{28}H_{31}N_3O_4$: C, 71.02; H, 6.60; N, 8.87. Found: C, 70.77; H, 6.89; N, 8.64.

*4-[3-(2-Benzoyl-phenoxy)-2-hydroxy-propyl]-piperazine-1-carbothioic Acid p-Tolylamide (**22**).* First, 200 mg (0.58 mmol) of [2-(2-hydroxy-3-piperazine-1-yl-propoxy)-phenyl]-phenyl-methanone (**5**) was dissolved in 10 mL of dichloromethane, and then a solution of 91 mg (0.61 mmol) of 4-methyl phenyl isothiocyanate in dichloromethane was added dropwise. The mixture was stirred at room temperature and monitored by TLC. After evaporation to dryness, yellow oil was obtained, which was further purified by column chromatography (silica gel, $CH_2Cl_2$/methanol/concentrated $NH_3$, 100/10/1). Subsequent removal of the solvents under reduced pressure yielded 181 mg (62.92%) of a light-yellow oil. $^1$H NMR ($CDCl_3$) $\delta$ 2.12−2.20 (m, 2H, $CH_2$-N), 2.33 (s, 3H, $CH_3$), 3.39−2.47 (m, 4H, *N*-$(CH_2)_2$), 3.74−3.79 (m, 5H, $(CH_2)_2$-N, CH), 3.96 (d, 2H, $J$ = 4.9, O-$CH_2$), 6.96−7.80 (m, 14H, arom H, NH). $^{13}$C NMR ($CDCl_3$) $\delta$ 20.89 ($CH_3$), 49.02 (*N*-$(CH_2)_2$), 52.55 ($(CH_2)_2$-N), 59.78 ($CH_2$-N), 65.88 (CH), 70.74 (O-$CH_2$), 112.73, 121.15, 123.47, 125.45, 128.31, (arom C), 128.71 (Ar-CO), 129.53, 129.63, 130.12, 132.38, 132.93 (arom H), 135.11 (Ar-$CH_3$), 137.34 (NH-Ar), 138.25 (Ph-CO), 156.51 (arom CO), 183.26 (CS), 196.47 (CO). MS $m/e$ 489.5 (M, 15%). Anal. Calcd for $C_{28}H_{31}N_3O_3S$: C, 68.69; H, 6.38; N, 8.58. Found: C, 68.60; H, 6.53; N, 8.47.

*[2-(3-{Benzoyl-phenoxy)-2-hydroxyl-propyl]-piperazine-1-yl}-2-hydroxy-propoxy)-phenyl]-phenyl-methanone (**23**).* First, 356 mg (1.40 mmol) of (2-oxiranylmethoxy-phenyl)-phenyl-methanone (**2a**) was dissolved in 20−30 mL of methanol and then 50.8 mg (0.59 mmol) of piperazine was added and the reaction mixture was refluxed for 5 h. Then after removal of the solvent by rotary evaporation, a column chromatography was performed (silica gel, $CH_2Cl_2$/methanol/concentrated $NH_3$, 100/10/1). Subsequent evaporation to dryness gave yellow oil, which crystallized from isopropyl alcohol to leave 424 mg (51%) of white solid; mp 125−135 °C. $^1$H NMR ($CDCl_3$) $\delta$ 1.98−2.42 (m, 12H, $CH_2$-*N*-$(CH_2)_2$-N-$CH_2$), 3.10 (s, 1H, OH), 3.70−3.76 (m, 2H, 2CH), 3.94−4.07 (m, 5H, O-$CH_2$, OH), 6.99−7.83 (m, 18H, arom H). $^{13}$C NMR ($CDCl_3$) $\delta$ 53.13 (*N*-$(CH_2)_4$-N), 60.06 ($CH_2$-NH), 65.47 (CH), 70.78 (O-$CH_2$), 112.62, 121.10, 128.28, 129.53, 130.09, 132.33, 132.82 (arom C), 128.81 (Ar-CO), 138.34 (Ph-CO), 156.55 (Ar-O), 196.46 (CO). MS $m/e$ 594.7 (M, 100%). Anal. Calcd for $C_{36}H_{38}N_2O_6$: C, 70.57; H, 7.14; N, 4.22. Found: C, 70.91; H, 7.02; N, 4.26.

*1-[2-(3-{4-[3-(2-Benzoyl-phenoxy)-2-hydroxyl-propyl]-piperazine-1-yl}-2-hydroxy-propoxy)-5-methyl-phenyl]-ethanone (**24**).* First, 500 mg (2.43 mmol) of 1-(5-methyl-2-oxiranylmethoxy-phenyl)-ethanone (**4**) was dissolved in 10 mL of methanol, treated with 857.1 mg (2.52 mmol) of [2-(2-hydroxy-3-piperazine-1-yl-propoxy)-phenyl]-phenyl-methanone (**5**), and refluxed for 5 h. Then after removal of solvent under reduced pressure, a column chromatography was performed (silica gel, $CH_2Cl_2$/methanol/concentrated $NH_3$, 120/10/1). Subsequent removal of the solvents under reduced pressure yielded 1.20 g (90.67%) of an orange oil: mp 89−93 °C. $^1$H NMR ($CDCl_3$) $\delta$ 2.05−2.13 (m, 2H, $CH_2$-N), 2.29 (s, 3H, $CH_3$), 2.33−2.55 (m, 10H, N-$(CH_2)_4$-N-$CH_2$), 2.62 (s, 3H, CO-$CH_3$), 2.98−3.01 (m, 1H, OH), 3.69−4.10 (m, 6H, 2O-$CH_2$-CH), 6.83−7.80 (m, 12H, arom H). $^{13}$C NMR ($CDCl_3$) $\delta$ 20.22 ($CH_3$-Ar), 31.81 ($CH_3$-CO), 53.20 (N-$(CH_2)_2$), 60.03, 60.49 (N-$CH_2$), 65.43, 65.51 (CH), 70.75, 71.12 (O-$CH_2$), 128.03, 128.82 (Ar-CO), 130.25 ($CH_3$-Ar), 112.61, 112.79, 121.10, 128.27, 129.51, 130.08, 130.59, 132.32, 132.81, 134.12 (arom C), 138 (Ph-CO), 156.00, 156.55 (Ar-O), 196.46 (CO), 199.88 (Ar-CO-$CH_3$). MS $m/e$ 594.7 (M+, 100%). Anal. Calcd for $C_{32}H_{38}N_2O_6$: C, 61.82; H, 6.65; N, 4.51. Found: C, 61.60; H, 6.91; N, 4.37.

**Computational Studies.** *Ligand Efficiency (LE).* Ligand efficiency (LE = $\Delta g$) values of the data were calculated by normalizing binding free energy of a ligand for number of heavy atoms. Free energy calculation was carried out as described by Hopkins et al. (eq 3). According to Hopkins et al., $IC_{50}$ from percentage inhibition can be substituted for *K*d (dissociation constant potency)[48] which was further confirmed by experimental results of Kuntz and co-workers.[38]

$$\Delta G = -RT \ln K_d \quad (3)$$

Ligand efficiency calculations was done for a temperature of 310 K and given in kcal per heavy atom (eq 4).

$$LE = (\Delta g) = -\Delta G/HA_{(\text{non-hydrogen atom})} \quad (4)$$


dx.doi.org/10.1021/jm201705f | J. Med. Chem. 2012, 55, 3261−3273

A size independent fit quality score was obtained as described by Reynolds et al.[21] by fitting the maximum LE over a large range of molecular size. All calculations regarding ligand efficiency were done by using Excel spreadsheet. $IC_{50}$ values of the propafenone type inhibitors (GPV576, GPV005, GPV062, and propafenone) were determined experimentally by a daunorubicin efflux essay.[37,49] Inhibition of rhodamine 123 efflux in the transfectant mouse lymphoma line L5178 VMDR1 C.06 were used to characterize the MDR-modulating activity values of verapamil, niguldipine, and cyclosporine A. $IC_{50}$ values of tariquidar,[50] elacridar,[51,52] valdapodar,[53] zosuquidar,[54,55] and ONT-093[56] were taken from literature (Table 2). $IC_{50}$ values for most of the compounds in clinical studies were reported by using rhodamine 123 efflux essays. We use these values, as there is a direct correlation between the $IC_{50}$ values from daunorubicin and rhodamine 123 efflux essays.[57]

*Lipophilic Efficiency (LipE).* LipE of benzophenones were calculated (eq 5) and compared with the compounds which reached clinical studies (verapamil, tariquidar, valspodar, elacridar, zosuquidar, ONT-093, niguldipine, and cyclosporine A) as well as with selected propafenone analogues.

$$\text{LipE} = \text{LLE} = \text{pIC}_{50} - \text{clogP} \quad (5)$$

clogP values of the data set were computed by using the Bio-Loom software package,[35] and the LipE calculations were performed by using Excel spreadsheet. To compare the standard threshold of LipE along three different entry pathways of ligands into respective binding pockets of P-gp, hERG and SERT, a data set from literature was used. It includes 744 SERT inhibitors extracted from the ChEMBL database,[40] 313 hERG blockers[41] from literature, and 372 inhibitors of P-gp mediated daunorubicin efflux (in-house data). The data sets are available at our homepage (pharminfo.univie.ac.at) and from Chemspider (www.chemspider.com).

**Docking.** Compounds **6**, **19**, **20**, and **23** were docked in their neutral form into an open state homology model of human P-gp[17] based on the X-ray structure of mouse P-gp (PDB: 3G5U)[19] by using the software package GOLD. To avoid any bias, we considered the whole transmembrane domain region as binding pocket. Then 100 poses per ligand were obtained, and finally ligand protein complexes were minimized by LigX, a minimization tool implemented in MOE, by using the MMFF94 force field.

A complete work flow of poses selection has been provided in Supporting Information (SM Workflow 1). Briefly, agglomerative Hierarchical Cluster analysis of the consensus rmsd matrix based on the common scaffold of the ligands identified two interesting clusters of poses containing all four ligands. However, additional five clusters have been identified containing three out of four ligands. All seven clusters were occupying the center of the binding cavity mainly interacting with amino acid residues of TM 1, 5, 6, 7, 8, 10, and 11 (SM Figure 2A). For a more detailed analysis of the ligand−protein interaction profiles of selected ligands, we used the two clusters containing all four ligands (SM Figure 2B).

To prioritize among the two clusters, a rescoring of all docking poses by using four different scoring functions in MOE (ASE, affinity dG, Alpha HB, London dG) was performed. Subsequently, for each ligand, the top 10 ranked poses according to consensus scoring were taken and analyzed. Out of these 40 poses, seven poses were present in cluster 1 while only one showed up in cluster 2. In addition, taking only the top ranked pose per ligand, two (**6**, **23**) out of four ligands were located in cluster 1 (SM Figure 2B). Additionally, cluster 1 was supported by photo affinity labeling and SAR data of the series. Therefore interaction position of cluster 1 was supposed to be the most likely one for benzophenones.

**Biological Assay.** *Cell Lines.* The resistant CCRF vcr1000 cell line was maintained in RPMI 1640 medium containing 10% fetal calf serum (FCS) and 1000 ng/mL vincristine. The selecting agent was washed out 1 week before the experiments. This cell line was selected due to its distinct P-gp expression.

*Inhibition of Daunorubicin Efflux.* $IC_{50}$ values for daunorubicin efflux inhibition were determined as reported.[32] Internal concentration (3 $\mu$M) of daunorubicin in the efflux inhibition assays was identified at least an order of magnitude below the $K_m$ values published for P-gp.[58,59]

Briefly, cells were sedimented, the supernatant was removed by aspiration, and the cells were resuspended at a density of $1 \times 10^6$/mL in RPMI 1640 medium containing daunorubicin (Sigma Chemical Co., St. Louis, MO) at a final concentration of 3 $\mu$mol/L. Cell suspensions were incubated at 37 °C for 30 min. Tubes were chilled on ice and centrifuged at 500*g* in an Eppendorf 5403 centrifuge (Eppendorf, Hamburg, Germany). Supernatants were removed, and the cell pellet was resuspended in medium prewarmed to 37 °C containing either no inhibitor or compounds at various concentrations ranging from 20 to 200 $\mu$M, depending on the solubility and expected potency of the inhibitor. Eight concentrations (serial 1:3 dilution) were tested for each inhibitor. After 60, 120, 180, and 240 s, aliquots of the incubation mixture were transferred to tubes containing an equal volume of ice-cold stop solution (RPMI medium containing GPV31 at a final concentration of 5 $\mu$mol/L). Zero time points were determined by immediately pipetting daunorubicin-preloaded cells into ice-cold stop solution. Samples drawn at the respective time points were kept in an ice water bath and measured within 1 h on a Becton Dickinson FACS Calibur flow cytometer (Becton Dickinson, Vienna, Austria). Viable cells were selected by setting appropriate gates for forward and side scatter. The excitation and emission wavelengths were 482 and 558 nm, respectively. Five thousand gated events were accumulated for the determination of mean fluorescence values.

## ■ ASSOCIATED CONTENT

### Ⓢ Supporting Information

LipE profiles of inhibitors of P-gp, SERT, and hERG; docking workflow; clustered docking poses; overlap of interacting amino acid residues of propafenone-type inhibitors of P-gp; photolabeled drug binding domains of propafenone-type inhibitors of P-gp. This material is available free of charge via the Internet at http://pubs.acs.org.

### Accession Codes

PDB ID: 3G5U.

## ■ AUTHOR INFORMATION

### Corresponding Author

*Phone: +43-1-4277-55110. Fax: +43-1-4277-9551. E-mail: gerhard.f.ecker@univie.ac.at.

### Notes

The authors declare no competing financial interest.

## ■ ACKNOWLEDGMENTS

We are grateful to the Austrian Science Fund for financial support (grant SFB F35). Ishrat Jabeen thanks the Higher Education Commission of Pakistan for financial support.

## ■ ABBREVIATIONS USED

P-gp, P-glycoprotein; LipE, lipophilic efficiency; LE, ligand efficiency; MDR, multidrug resistance; ABC, ATP binding cassette; QSAR, quantitative structure−activity relationship

## ■ REFERENCES

(1) Giacomini, K. M.; Huang, S. M.; Tweedie, D. J.; Benet, L. Z.; Brouwer, K. L.; Chu, X.; Dahlin, A.; Evers, R.; Fischer, V.; Hillgren, K. M.; Hoffmaster, K. A.; Ishikawa, T.; Keppler, D.; Kim, R. B.; Lee, C. A.; Niemi, M.; Polli, J. W.; Sugiyama, Y.; Swaan, P. W.; Ware, J. A.; Wright, S. H.; Yee, S. W.; Zamek-Gliszczynski, M. J.; Zhang, L. Membrane transporters in drug development. *Nature Rev. Drug Discovery* **2010**, *9*, 215−236.

(2) Lee, E. J.; Lean, C. B.; Limenta, L. M. Role of membrane transporters in the safety profile of drugs. *Expert Opin. Drug Metab. Toxicol* **2009**, *5*, 1369−1383.

(3) Szakacs, G.; Paterson, J. K.; Ludwig, J. A.; Booth-Genthe, C.; Gottesman, M. M. Targeting multidrug resistance in cancer. *Nature Rev. Drug Discovery* **2006**, *5*, 219−234.
(4) Couture, L.; Nash, J. A.; Turgeon, J. The ATP-binding cassette transporters and their implication in drug disposition: a special look at the heart. *Pharmacol. Rev.* **2006**, *58*, 244−258.
(5) Szakacs, G.; Varadi, A.; Ozvegy-Laczka, C.; Sarkadi, B. The role of ABC transporters in drug absorption, distribution, metabolism, excretion and toxicity (ADME-Tox). *Drug Discovery Today* **2008**, *13*, 379−393.
(6) Colabufo, N. A.; Berardi, F.; Contino, M.; Niso, M.; Perrone, R. ABC pumps and their role in active drug transport. *Curr. Top. Med. Chem.* **2009**, *9*, 119−129.
(7) Gottesman, M. M.; Ling, V. The molecular basis of multidrug resistance in cancer: the early years of P-glycoprotein research. *FEBS Lett.* **2006**, *580*, 998−1009.
(8) Glavinas, H.; Krajcsi, P.; Cserepes, J.; Sarkadi, B. The role of ABC transporters in drug resistance, metabolism and toxicity. *Curr. Drug Delivery* **2004**, *1*, 27−42.
(9) Juliano, R.; Ling, V.; Graves, J. Drug-resistant mutants of chinese hamster ovary cells possess an altered cell surface carbohydrate component. *J. Supramol. Struct.* **1976**, *4*, 521−526.
(10) Ford, R. C.; Kamis, A. B.; Kerr, I. D.; Callaghan, R. The ABC Transporters: Structural Insights into Drug Transport. In *Transporters as Drug Carriers*; Wiley-VCH Verlag GmbH & Co. KGaA: Weinheim, Germany, 2010; pp 1−48.
(11) Broccatelli, F.; Carosati, E.; Neri, A.; Frosini, M.; Goracci, L.; Oprea, T. I.; Cruciani, G. A Novel Approach for Predicting P-Glycoprotein (ABCB1) Inhibition Using Molecular Interaction Fields. *J. Med. Chem.* **2011**, *54*, 1740−1751.
(12) Kemper, E. M.; van Zandbergen, A. E.; Cleypool, C.; Mos, H. A.; Boogerd, W.; Beijnen, J. H.; van Tellingen, O. Increased penetration of paclitaxel into the brain by inhibition of P-Glycoprotein. *Clin. Cancer Res.* **2003**, *9*, 2849−2855.
(13) Kuhnle, M.; Egger, M.; Muller, C.; Mahringer, A.; Bernhardt, G.; Fricker, G.; Konig, B.; Buschauer, A. Potent and selective inhibitors of breast cancer resistance protein (ABCG2) derived from the p-glycoprotein (ABCB1) modulator tariquidar. *J. Med. Chem.* **2009**, *52*, 1190−1197.
(14) Ford, J. M. Experimental reversal of P-glycoprotein-mediated multidrug resistance by pharmacological chemosensitisers. *Eur. J. Cancer* **1996**, *32A*, 991−1001.
(15) Thomas, H.; Coley, H. M. Overcoming multidrug resistance in cancer: an update on the clinical strategy of inhibiting p-glycoprotein. *Cancer Control* **2003**, *10*, 159−165.
(16) Kannan, P.; John, C.; Zoghbi, S. S.; Halldin, C.; Gottesman, M. M.; Innis, R. B.; Hall, M. D. Imaging the function of P-glycoprotein with radiotracers: pharmacokinetics and in vivo applications. *Clin. Pharmacol. Ther.* **2009**, *86*, 368−377.
(17) Klepsch, F.; Chiba, P.; Ecker, G. F. Exhaustive sampling of docking poses reveals binding hypotheses for propafenone type inhibitors of P-glycoprotein. *PLoS Comput. Biol.* **2011**, *7*, e1002036.
(18) Sharom, F. J. The P-glycoprotein multidrug transporter. *Essays Biochem.* **2011**, *50*, 161−178.
(19) Aller, S. G.; Yu, J.; Ward, A.; Weng, Y.; Chittaboina, S.; Zhuo, R.; Harrell, P. M.; Trinh, Y. T.; Zhang, Q.; Urbatsch, I. L.; Chang, G. Structure of P-glycoprotein reveals a molecular basis for poly-specific drug binding. *Science* **2009**, *323*, 1718−1722.
(20) Andrews, P. R.; Craik, D. J.; Martin, J. L. Functional group contributions to drug−receptor interactions. *J. Med. Chem.* **1984**, *27*, 1648−1657.
(21) Reynolds, C. H.; Bembenek, S. D.; Tounge, B. A. The role of molecular size in ligand efficiency. *Bioorg. Med. Chem. Lett.* **2007**, *17*, 4258−4261.
(22) Reynolds, C. H.; Tounge, B. A.; Bembenek, S. D. Ligand binding efficiency: trends, physical basis, and implications. *J. Med. Chem.* **2008**, *51*, 2432−2438.
(23) Leeson, P. D.; Springthorpe, B. The influence of drug-like concepts on decision-making in medicinal chemistry. *Nature Rev. Drug Discovery* **2007**, *6*, 881−890.
(24) Ryckmans, T.; Edwards, M. P.; Horne, V. A.; Correia, A. M.; Owen, D. R.; Thompson, L. R.; Tran, I.; Tutt, M. F.; Young, T. Rapid assessment of a novel series of selective CB(2) agonists using parallel synthesis protocols: a lipophilic efficiency (LipE) analysis. *Bioorg. Med. Chem. Lett.* **2009**, *19*, 4406−4409.
(25) Keseru, G. M.; Makara, G. M. The influence of lead discovery strategies on the properties of drug candidates. *Nature Rev. Drug Discovery* **2009**, *8*, 203−212.
(26) Mortenson, P. N.; Murray, C. W. Assessing the lipophilicity of fragments and early hits. *J. Comput.-Aided Mol. Des.* **2011**, *25*, 663−667.
(27) Chiba, P.; Burghofer, S.; Richter, E.; Tell, B.; Moser, A.; Ecker, G. Synthesis, pharmacologic activity, and structure−activity relationships of a series of propafenone-related modulators of multidrug resistance. *J. Med. Chem.* **1995**, *38*, 2789−2793.
(28) Kaiser, D.; Smiesko, M.; Kopp, S.; Chiba, P.; Ecker, G. F. Interaction field based and hologram based QSAR analysis of propafenone-type modulators of multidrug resistance. *Med. Chem.* **2005**, *1*, 431−444.
(29) Ecker, G. F.; Csaszar, E.; Kopp, S.; Plagens, B.; Holzer, W.; Ernst, W.; Chiba, P. Identification of ligand-binding regions of P-glycoprotein by activated-pharmacophore photoaffinity labeling and matrix-assisted laser desorption/ionization-time-of-flight mass spectrometry. *Mol. Pharmacol.* **2002**, *61*, 637−648.
(30) Parveen, Z.; Stockner, T.; Bentele, C.; Pferschy, S.; Kraupp, M.; Freissmuth, M.; Ecker, G. F.; Chiba, P. Molecular Dissection of Dual Pseudosymmetric Solute Translocation Pathways in Human P-Glycoprotein. *Mol. Pharmacol.* **2011**, *79*, 443−452.
(31) Pitha, J.; Szabo, L.; Szurmai, Z.; Buchowiecki, W.; Kusiak, J. W. Alkylating prazosin analogue: irreversible label for alpha 1-adrenoceptors. *J. Med. Chem.* **1989**, *32*, 96−100.
(32) Chiba, P.; Ecker, G.; Schmid, D.; Drach, J.; Tell, B.; Goldenberg, S.; Gekeler, V. Structural requirements for activity of propafenone-type modulators in P-glycoprotein-mediated multidrug resistance. *Mol. Pharmacol.* **1996**, *49*, 1122−1130.
(33) Tmej, C.; Chiba, P.; Huber, M.; Richter, E.; Hitzler, M.; Schaper, K. J.; Ecker, G. A combined Hansch/Free-Wilson approach as predictive tool in QSAR studies on propafenone-type modulators of multidrug resistance. *Arch. Pharm. (Weinheim, Ger.)* **1998**, *331*, 233−240.
(34) König, G.; Chiba, P.; Ecker, G. F. Hydrophobic moments as physicochemical descriptors in structure−activity relationship studies of P-glycoprotein inhibitors. *Monatsh. Chem.* **2008**, *139*, 401−405.
(35) Bio-Loom program, trial version, by BioByte Co.
(36) Sakuratani, Y.; Kasai, K.; Noguchi, Y.; Yamada, J. Comparison of Predictivities of Log P Calculation Models Based on Experimental Data for 134 Simple Organic Compounds. *QSAR Comb. Sci.* **2007**, *26*, 109−116.
(37) Chiba, P.; Hitzler, M.; Richter, E.; Huber, M.; Tmej, C.; Giovagnoni, E.; Ecker, G. Studies on Propafenone-Type Modulators of Multidrug Resistance III: Variations on the Nitrogen. *Quant. Struct.-Act. Relat.* **1997**, *16*, 361−366.
(38) Kuntz, I. D.; Chen, K.; Sharp, K. A.; Kollman, P. A. The maximal affinity of ligands. *Proc. Natl. Acad. Sci. U.S.A* **1999**, *96*, 9997−10002.
(39) Verdonk, M. L.; Rees, D. C. Group efficiency: a guideline for hits-to-leads chemistry. *ChemMedChem* **2008**, *3*, 1179−1180.
(40) *ChEMBLdb*; https://www.ebi.ac.uk/chembldb/ (Accessed April 2010).
(41) Thai, K. M.; Ecker, G. F. A binary QSAR model for classification of hERG potassium channel blockers. *Bioorg. Med. Chem.* **2008**, *16*, 4107−4119.
(42) Wellfelt, K.; Skold, A. C.; Wallin, A.; Danielsson, B. R. Teratogenicity of the class III antiarrhythmic drug almokalant. Role of hypoxia and reactive oxygen species. *Reprod. Toxicol.* **1999**, *13*, 93−101.

(43) Houltz, B.; Darpo, B.; Swedberg, K.; Blomstrom, P.; Brachmann, J.; Crijns, H. J.; Jensen, S. M.; Svernhage, E.; Vallin, H.; Edvardsson, N. Effects of the Ikr-blocker almokalant and predictors of conversion of chronic atrial tachyarrhythmias to sinus rhythm. A prospective study. *Cardiovasc. Drugs Ther.* **1999**, *13*, 329−338.
(44) Jabeen, I.; Wetwitayaklung, P.; Klepsch, F.; Parveen, Z.; Chiba, P.; Ecker, G. F. Probing the stereoselectivity of P-glycoprotein-synthesis, biological activity and ligand docking studies of a set of enantiopure benzopyrano[3,4-*b*][1,4]oxazines. *Chem. Commun. (Cambridge, U.K.)* **2011**, *47*, 2586−2588.
(45) Pajeva, I.; Wiese, M. Molecular modeling of phenothiazines and related drugs as multidrug resistance modifiers: a comparative molecular field analysis study. *J. Med. Chem.* **1998**, *41*, 1815−1826.
(46) Pleban, K.; Kopp, S.; Csaszar, E.; Peer, M.; Hrebicek, T.; Rizzi, A.; Ecker, G. F.; Chiba, P. P-Glycoprotein substrate binding domains are located at the transmembrane domain/transmembrane domain interfaces: a combined photoaffinity labeling-protein homology modeling approach. *Mol. Pharmacol.* **2005**, *67*, 365−374.
(47) Chiba, P.; Mihalek, I.; Ecker, G. F.; Kopp, S.; Lichtarge, O. Role of transmembrane domain/transmembrane domain interfaces of P-glycoprotein (ABCB1) in solute transport. Convergent information from photoaffinity labeling, site directed mutagenesis and in silico importance prediction. *Curr. Med. Chem.* **2006**, *13*, 793−805.
(48) Hopkins, A. L.; Groom, C. R.; Alex, A. Ligand efficiency: a useful metric for lead selection. *Drug Discovery Today* **2004**, *9*, 430−431.
(49) Pleban, K.; Hoffer, C.; Kopp, S.; Peer, M.; Chiba, P.; Ecker, G. F. Intramolecular distribution of hydrophobicity influences pharmacological activity of propafenone-type MDR modulators. *Arch. Pharm. (Weinheim, Ger.)* **2004**, *337*, 328−334.
(50) Roe, M.; Folkes, A.; Ashworth, P.; Brumwell, J.; Chima, L.; Hunjan, S.; Pretswell, I.; Dangerfield, W.; Ryder, H.; Charlton, P. Reversal of P-glycoprotein mediated multidrug resistance by novel anthranilamide derivatives. *Bioorg. Med. Chem. Lett.* **1999**, *9*, 595−600.
(51) Dodic, N.; Dumaitre, B.; Daugan, A.; Pianetti, P. Synthesis and activity against multidrug resistance in Chinese hamster ovary cells of new acridone-4-carboxamides. *J. Med. Chem.* **1995**, *38*, 2418−2426.
(52) Bachmeier, C. J.; Miller, D. W. A fluorometric screening assay for drug efflux transporter activity in the blood−brain barrier. *Pharm. Res.* **2005**, *22*, 113−121.
(53) Wang, J. S.; Zhu, H. J.; Markowitz, J. S.; Donovan, J. L.; DeVane, C. L. Evaluation of antipsychotic drugs as inhibitors of multidrug resistance transporter P-glycoprotein. *Psychopharmacology (Berlin, Ger.)* **2006**, *187*, 415−423.
(54) Shepard, R. L.; Cao, J.; Starling, J. J.; Dantzig, A. H. Modulation of P-glycoprotein but not MRP1- or BCRP-mediated drug resistance by LY335979. *Int. J. Cancer* **2003**, *103*, 121−125.
(55) Dantzig, A. H.; Shepard, R. L.; Cao, J.; Law, K. L.; Ehlhardt, W. J.; Baughman, T. M.; Bumol, T. F.; Starling, J. J. Reversal of P-glycoprotein-mediated multidrug resistance by a potent cyclopropyldibenzosuberane modulator, LY335979. *Cancer Res.* **1996**, *56*, 4171−4179.
(56) Newman, M. J.; Rodarte, J. C.; Benbatoul, K. D.; Romano, S. J.; Zhang, C.; Krane, S.; Moran, E. J.; Uyeda, R. T.; Dixon, R.; Guns, E. S.; Mayer, L. D. Discovery and characterization of OC144-093, a novel inhibitor of P-glycoprotein-mediated multidrug resistance. *Cancer Res.* **2000**, *60*, 2964−2972.
(57) Chiba, P.; Holzer, W.; Landau, M.; Bechmann, G.; Lorenz, K.; Plagens, B.; Hitzler, M.; Richter, E.; Ecker, G. Substituted 4-acylpyrazoles and 4-acylpyrazolones: synthesis and multidrug resistance-modulating activity. *J. Med. Chem.* **1998**, *41*, 4001−4011.
(58) Ayesh, S.; Shao, Y. M.; Stein, W. D. Co-operative, competitive and non-competitive interactions between modulators of P-glycoprotein. *Biochim. Biophys. Acta* **1996**, *1316*, 8−18.
(59) Shao, Y. M.; Ayesh, S.; Stein, W. D. Mutually co-operative interactions between modulators of P-glycoprotein. *Biochim. Biophys. Acta* **1997**, *1360*, 30−38.